CONF-890665--18

SAND--88-3437C

DE89 013815

INTERSTAGE CLOSURE TIMES FOR THE RIMFIRE MULTISTAGE GAS SWITCH*

B. N. Turman and D. R. Humphreys
Sandia National Laboratories
Albuquerque, NM 87185
and
C. N. Richards
Atmospheric Physics Associates
Peralta, NM 87042

Abstract

The Rimfire multistage switch is a low-jitter SF_6 insulated gas switch that has been developed for PBFA II. The first stage is laser-triggered, and the subsequent stages are self-fired by the over-voltage from the closure of the triggered stage. The runtime of the 5 MV PBFA II switch is approximately 30 ns, and the standard deviation timing jitter is 1 ns. A Thomson streak camera and cylindrical imaging optics have been used to observe stage closure times, and a gated, single-frame camera recorded snapshots of the discrete arcs during closure. These observations have shown that approximately half the switch closure time comes from the trigger and first self-break gap. The switch jitter is also dominated by these first gaps. Computer simulations, based on T. H. Martin's empirical gas breakdown model, agree with the experimental measurements, and give insight to the dynamics of the switch closure process.

Introduction

The Rimfire multistage switch is a low-jitter SF_6-insulated gas switch that has been developed for PBFA II. The switch is shown schematically in Fig. 1. This switch is triggered with a KrF laser with 22 ns FWHM (40 ns total width) and is designed for 5-MV operation at an average field of approximately 230 kV/cm with 60-70 psia pressure.[1,2,3] Figure 2 gives the electric field profile across the switch in the field-graded environment of PBFA II and Demon, the prototype demonstration module for PBFA II. Several field distributions have been tested during the development of this switch; Figure 2 shows the two principal solutions that have been evaluated operationally both on Demon and PBFA II. The high-voltage electrodes of this multistage switch are isolated from the external water environment to reduce interstage capacitance and minimize tracking at the water-plastic interface that would otherwise occur as a result of high-voltage transients generated during closure. The first stage is laser-triggered, and the subsequent stages are self-fired by the overvoltage from the closure of the triggered stage. The trigger stage is formed with spherically-contoured, low field-enhancement electrodes with a 4.5-cm gap. The self-break gaps are formed with disk-shaped electrodes separated by 0.9-cm gaps and supported by plastic insulators at the axis of the switch.

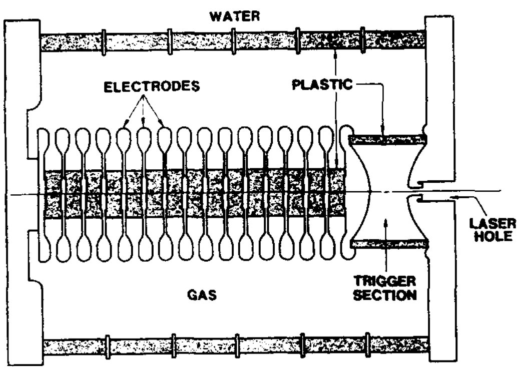

Figure 1. Schematic drawing of the Rimfire switch.

*This work was sponsored by the U.S. Department of Energy under Contract Number DE-AC04-76DP00789.

Since the original development of this switch for PBFA II, other variations have been developed for application on Saturn, Radlac II, Mite, Aurora, and Hermes III, for 4-MV and 3-MV operation.

Previous studies have evaluated the self-breakdown, insulator flashover, and timing jitter characteristics of this switch.[2,3] Optimal performance, with standard deviation timing jitter of 1 ns is obtained when the normalized trigger field is greater than

$$E_{trig}/P > 45 \text{ kV/cm-bar} \qquad (1)$$

The average field across the switch should not exceed the prefire limit by [2]

$$E/P \text{ (kV/cm-bar)} < 82 - 3.5\,P, \quad P \text{ in bars} \qquad (2)$$

The trigger field limit is approximately 70% of the self-breakdown field of the switch.

Additional study of this switch has been conducted to understand the detailed structure of the closure times of each stage, the parameters that affect these times, and the jitter of each stage. These results are the subject of the present paper.

Experimental Observations of Switch Closure Times

Figure 3 shows the Demon accelerator. The Rimfire switch is located between the intermediate store and the Line 1 water-switched pulse-forming line. A field-shaper on the end of the intermediate store produces the axial electric field distribution

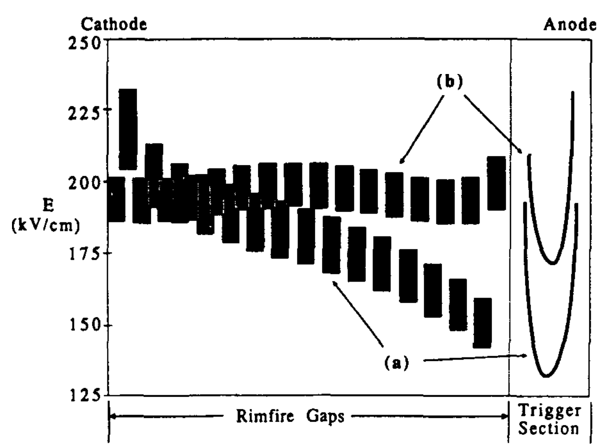

Figure 2. JASON electric field plots (at 3.8 MV) for two field-shaping modifications of the PBFA II Rimfire switch. Curve b is the version currently used in PBFA II.[3]

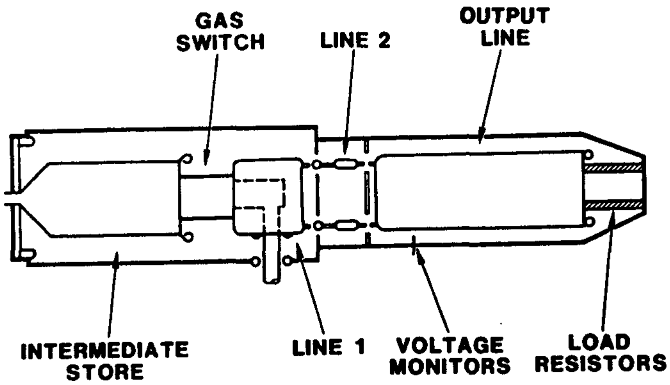

Figure 3. The Demon test configuration.

shown in Fig. 2. The Demon tank provides good visual access for switch photography, with an open top surface and view ports on two sides of the coaxial line. For this series of experiments, both of the field distributions of Fig. 2 were studied. The switch housings were the standard configuration for PBFA II, with the exception that the grooved-insulator walls of the switch envelope were replaced with clear polished straight wall insulators. These grooved-wall insulators add a significant flashover margin for the switch and increase its high-voltage reliability. However, unobstructed optical images could not be obtained with the grooved insulators. The straight wall insulators performed adequately at and below 5 MV, where this experiment was conducted.

A Thomson streak camera model 506 and cylindrical imaging optics were used to observe stage closure times, and a gated, single-frame camera recorded snapshots of the discrete arcs during closure (Fig. 4). An open-shutter camera was also used for a time-integrated record of the arc locations. The cameras were gated through a CAMAC timing system to the laser firing system. Electrical measurement of switch run time was obtained from V-dot monitors and correlated with the camera observations through the CAMAC system. The most crucial timing points were measured with 50-ps resolution CAMAC modules.

Figure 5 shows a time-integrated photograph of the closing switch. Note that the gap breakdown is characterized by a number of discrete arcs, distributed around the perimeter of the electrodes. The trigger stage forms a single arc, and the first self-break gap forms one or two arcs. The remaining gaps form an average of four arcs each. The gated camera shows that the stages break sequentially.

Table 1 summarizes the test parameters for four test series utilizing the two switch configurations from Fig. 2. Each test was composed of 10 to 30 shots. The intent of these tests was to bracket the interesting transition region of 45 kV/cm-bar below which the switch loses synchronization. The combined optical and electrical measurements allow us to determine the jitter distribution within the switch, as well as the run time of the individual stages. Measurement errors were determined from repeated measurements of laser pulse arrival times and measurements of a 25 Mhz optical time mark generator. The optical time mark generator was also superimposed on the shot streak photographs for sweep speed calibration. With the Thomson 506N "nanosecond" unit, measurement uncertainty of about 1.5 ns standard deviation was obtained. With the Thomson 506P "picosecond" unit, the measurement uncertainty was under 1 ns.

Interstage closure times are shown in Fig. 6. Standard deviation error bars are included on the graph. The start time for this figure is the arrival time of the laser trigger pulse. The total switch run time is plotted to the far right. Only 11 of the 16 gaps were visible in the experiment, but we can see that the closure time of the last visible gap is very near the electrically measured total closure time. The switch run time increases dramatically as the normalized trigger electric field decreases, in agreement with previous observations.[2] This increase comes from both the triggered section and the self-break section of the switch. The trigger and first self-break gap together account for almost half of the total run time.

Jitter measurements are summarized in Table 1. Total jitter was measured with the CAMAC timer, while the triggered-gap and self-break gap data were taken from repeated measurement from the streak camera. The subnanosecond jitter of test 2, with 45 kV/cm-bar, was below the measurement error for the optical system. Consequently, jitter data were not available for inter-stage jitter for test 2. The jitter values in Table 1 were calculated from

$$\sigma^2_{gap} = \sigma^2_{meas} - \sigma^2_{error} . \qquad (2)$$

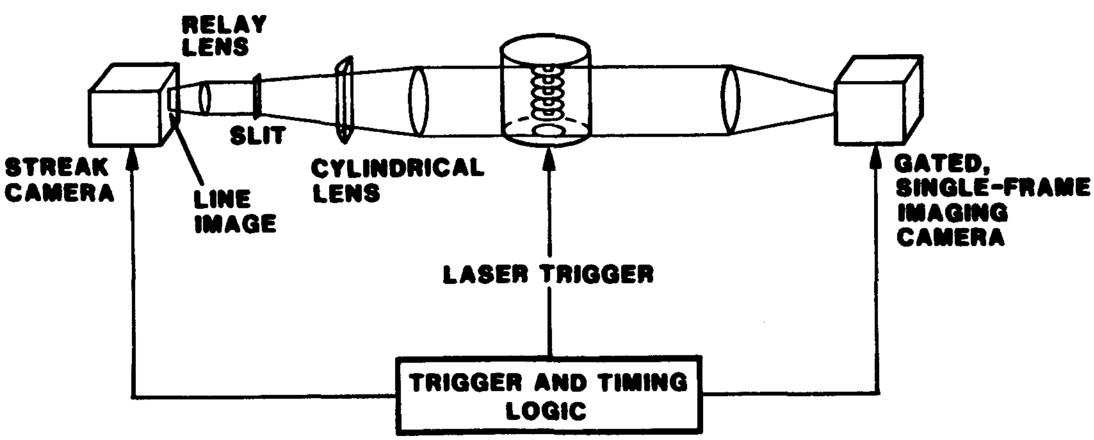

Figure 4. Streak camera, gated camera, and CAMAC timing are linked to provide experimental uncertainty of about 1 ns. The cylindrical lens forms a compressed image of the switch, focused on the slit plane.

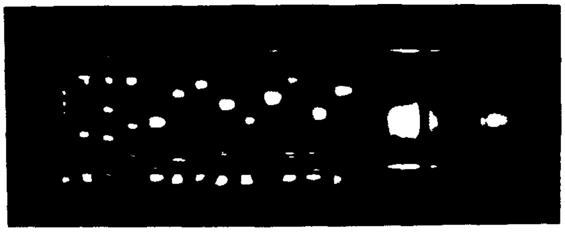

Figure 5. An open-shutter image of the switch. The triggered gap is at the far right. Multiple arcs are seen in the self-break gaps.

The measurement error was 1 ns for 506P data and 1.5 ns for 506N data. The sampling uncertainty for these jitter measurements is +0.5/-0.3 ns.

These data suggest that the increased jitter with lowered field or increased pressure grows approximately equally in the triggered and self-break gaps. The long delay time of the first self-break gap also suggests that this gap may contribute almost all of the jitter for the self-break gaps. This point is now being addressed in additional tests.

The normal operating laser energy for Demon and PBFA II is about 30 mJ per switch. In Test 4, we increased the trigger energy to 60 mJ with E_t/P of 39 kV/cm-bar. In comparison to Test 1, the jitter of the self-break gaps remained approximately constant, but the trigger gap jitter was significantly improved. Total jitter was reduced accordingly. Since the trigger gap closes faster than the laser pulse width of 40 ns, only a fraction of this energy is actually used in controlling the switch. A study of the laser energy and pulse width dependence for the Hermes III Rimfire switch is given in Reference [4].

Guenther and Bettis have shown that the jitter of a single-stage laser-triggered gap is abruptly degraded when the gap delay exceeds the laser pulse width.[5] This effect may be responsible for the increased jitter of Test 4, where the total switch run time has exceeded the laser pulse width. One might expect to see an even stronger increase in jitter when the run time of the triggered gap exceeds the laser pulse width. A shorter laser pulse width will be used in later experiments to look for this effect.

Computer Simulations

The non-linear closure of the switch gaps can be explained intuitively as a result of field enhancement as the first stages of the switch close.

Table 1
Test Summary

	Test 1	Test 2	Test 3	Test 4
Switch Configurations	a	b	b	b
Voltage Across Switch (MV)	3.6	4.5	4.0	4.1
Pressure (psia)	55	65	70	70
E_t/P (kV/cm-bar)	39	45	37	39
Laser Pulse Width (ns)	40	40	40	40
Switch Run Time (ns)	32	22	47	36
Total Jitter (ns)	2.1	0.6	2.9	1.3
Trigger Gap Jitter (ns)	1.5	---	1.6	1.0
Self-break Gap Jitter (ns)	1.0	---	1.7	< 1
Laser Energy (mJ)	30	30	30	60

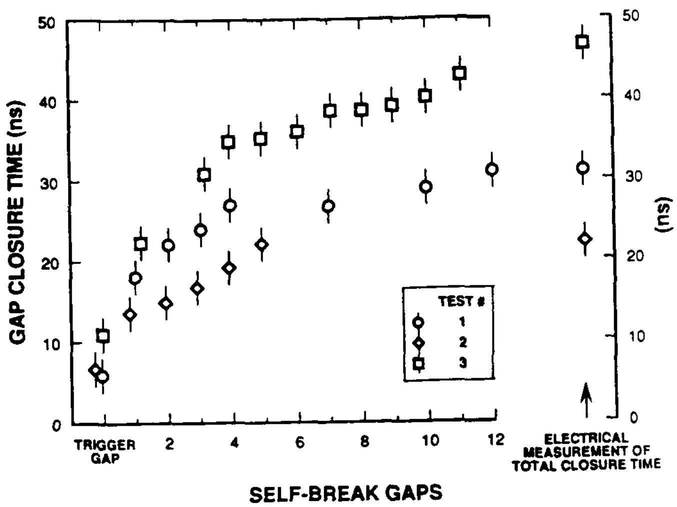

Figure 6. Gap closure data from streak camera measurements. Total closure time at the right of this figure is measured electrically.

Approximately 22 % of the total switch voltage is across the trigger gap. When this gap is closed by the laser spark, that voltage is redistributed across the remaining gaps, with the closest gap receiving a larger overstress than successive gaps. The increased voltage on the first gap accelerates the closure process; when that gap closes, its voltage is also redistributed to the successive gaps. Figure 7 is a two-dimensional electrostatic simulation of the Rimfire fields during closure. This simulation assumes that the first five self-break gaps have been closed and are conductive. Note that the electric field in the nearest unclosed gap is highly enhanced by the closed gaps. Since breakdown is highly dependent on voltage and field [6,7], successive gaps will break much faster than the previous. It is this enhancement that drives the switch toward rapid non-linear closure that is clearly seen in the experiments.

A computer simulation has been developed to model this closure process.[8]. The TUMBLE computer code is based on T. H. Martin's empirical model for gas breakdown, which gives the relation between breakdown time, voltage, gas pressure, and gap length over a wide range of parameters [6,7]. This model is developed in an integral formulation to accommodate voltage transients that develop during stage-to-stage closure [8]. The gap breakdown time t after streamer onset t_s is calculated from the integral

$$\int_{t_s}^{t} V^6 dt = K^6 \quad (3)$$

$$K = 260\, P^{0.56} d^{0.833} \text{ for } SF_6 .$$

V(t) is the voltage across the gap in kV, t is in ns, d is the gap length in cm, and P is the pressure in bars.

For triggered operation, t_s is the laser pulse arrival time. The laser spark is assumed to reduce the trigger gap by the length of the ionized spark. This parameter is determined from the streak photograph of the initial trigger spark.

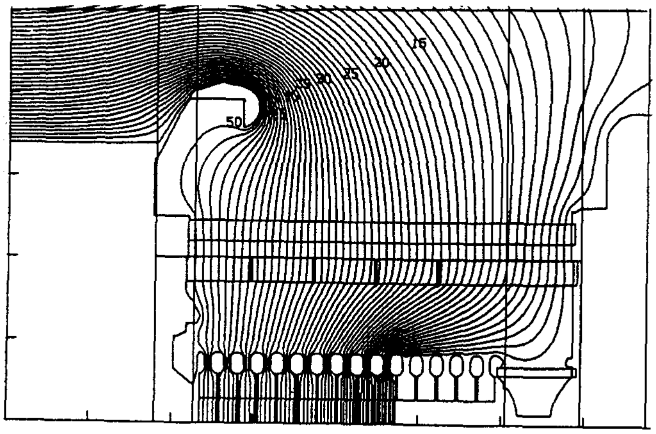

Figure 7. JASON electric field plot, wit the first five gaps assumed to be closed. Note: the high field concentrations on the unclosed gaps.

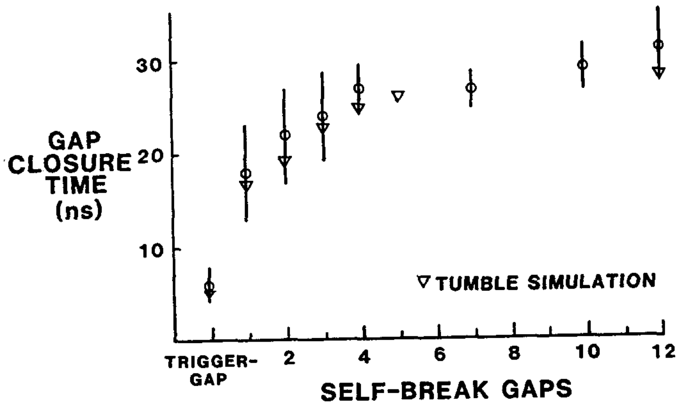

Figure 8. Comparison of TUMBLE calculation with gap closure data from Test 1.

The transient gap voltage function is calculated from an overvoltage matrix that was developed from JASON field plots such as Fig. 7, in which the sequential gap breakdowns were simulated. These overvoltages were modulated by high-frequency ringing of the switch as calculated from a two-dimensional electromagnetic simulation by W. A. Johnson [7]. Finally, the Demon charging waveform is assumed for the initial voltage waveform.

The resulting simulation is compared with the Test 1 experiment in Fig. 8. Table 2 compares experimental and model results for trigger gap and total run time for two tests. The computer model and experiment agree within 1 or 2 ns for the laser-triggered gap closure and within 7 ns for total closure time. This agreement tends to support the general picture of a breakdown voltage wave driving the closure of the switch. A fully self-consistent analysis, in which the breakdown formulation of Equation 3 is incorporated into an electromagnetic field-solving routine, would be useful for more generalized solutions.

Table 2
Comparison of Experimental and Model Results for Gap Closure

	Test 2		Test 3	
Gap	Experiment	Model	Experiment	Model
Trigger (ns)	7	6	11	15
Self-break 1 (ns)	13	12	22	21
Self-break 2 (ns)	15	13	29	25
Completion (ns)	23	22	47	40

Summary

Detailed study of the closure sequence of the Rimfire switch has been conducted with a fast streak camera, gated framing camera, and electrical measurement of switch conduction time and jitter. The experimental observations show a non-linear, but highly ordered closure sequence, in which more than half the Rimfire switch closure time comes from the trigger and first self-break gap. Over half of the switch jitter comes from the trigger gap. A computer simulation was developed with the assumption that field enhancement from the triggered-gap closure drives the closure of the later stages and thus accounts for the non-linear nature of the switch closure. This assumption, with the Martin gap closure model, gives good agreement with data.

Acknowledgements

We wish to acknowledge the experimental support of Wes Helgeson, Frank Morgan, Mark Herman, Mick Butler, and Gary Pena in the operation of Demon and the associated camera equipment. Also, T. H. Martin, D. D. Bloomquist, and W. A. Johnson aided in analysis and computer support.

References

[1] D. R. Humphreys, K. J. Penn, J. S. Cap, R. G. Adams, J. F. Seamen, and B. N. Turman, "Rimfire: A Six Megavolt Laser-Triggered Gas Filled Switch for PBFA II," in Proceedings of the 5th IEEE Pulsed Power Conference, Arlington, VA, June 1987, pp. 262-265.

[2] B. N. Turman and D. R. Humphreys, "Scaling Relations for the Rimfire Multi-Stage Gas Switch," in Proceedings of the 6th IEEE Pulsed Power Conference, Arlington, VA, June 1987, pp. 347-353.

[3] J. M. Wilson and G. L. Donovan, "Laser-Triggered Gas Switch Improvements on PBFA II," in Proceedings of the 6th IEEE Pulsed Power Conference, Arlington, VA, June 1987, pp. 361-364.

[4] G. J. Denison, "Hermes III High-Voltage, Multistage, Laser-Triggered Gas Switch," presented at the 7th IEEE Pulsed Power Conference, Monterey, CA, June 11-14, 1989.

[5] A. H. Guenther and J. R. Bettis, "The Laser Triggering of High-Voltage Switches," J. Phys. D: Appl. Phys., vol. 11, pp. 1577-1613, 1978.

[6] T. H. Martin, "Pulse Charged Gas Breakdown," in Proceedings of the 5th IEEE Pulsed Power Conference, Arlington, VA, June 1985, pp. 74-83.

[7] T. H. Martin, "An Empirical Formula for Gas Switching," presented at the 7th IEEE Pulsed Power Conference, Monterey, CA, June 11-14, 1989.

[8] B. N. Turman, D. R. Humphreys, and R. G. Adams, "Trigger Delay Time Modeling for the Rimfire Switch," SAND86-0015, Particle Beam Fusion Progress Report Jan. 1985 through June 1985, June 1986, pp. 81-82.

[9] W. A. Johnson, D. B. Seidel, and D. R. Humphreys, "A MAGIC Simulation of a 6-MV Rimfire Gas Switch," SAND86-0016, Particle Beam Fusion Progress Report July 1985 through Dec. 1985, Dec. 1987, pp. 136-138.